Nanoscale Res Lett (2010) 5:533–538
DOI 10.1007/s11671-010-9542-0

SPECIAL ISSUE ARTICLE

Biomolecules Detection Using a Silver-Enhanced Gold Nanoparticle-Based Biochip

Yang Liu · Deng Zhang · Evangelyn C. Alocilja · Shantanu Chakrabartty

Received: 30 September 2009 / Accepted: 16 January 2010 / Published online: 2 February 2010

Abstract Silver-enhanced labeling method has been employed in immunochromatographic assays for improving the sensitivity of detecting pathogens. In this paper, we apply the silver enhancement technique for biomolecular signal amplification in a gold nanoparticle-based conductimetric biochip. We show that the response of the silver-enhanced biochip comprises two distinct regions namely: (a) a sub-threshold region where conduction occurs due to electron hopping between silver islands and the electrolyte and (b) an above-threshold region where the conduction is due to a direct flow of electrons. These two regions are characterized by different conduction slopes, and we show that combining the information from both these regions can improve the sensitivity of the biochip. Results from fabricated prototypes show a dynamic range of more than 40 dB and with a detection limit less than 240 pg/mL. The fabrication of the biochip is compatible with standard complementary metal–oxide–semiconductor (CMOS) processes making it ideal for integration in next-generation CMOS biosensors.

Keywords Gold nanoparticle · Silver enhancement · Biomolecules · Biochip · Biosensor

Y. Liu (✉) · S. Chakrabartty
Electrical and Computer Engineering, Michigan State University, East Lansing, MI 48824, USA
e-mail: liuyang4@egr.msu.edu

D. Zhang · E. C. Alocilja
Biosystems and Agricultural Engineering, Michigan State University, East Lansing, MI 48824, USA

Introduction

Biosensors have emerged as important analytical tools for detecting and controlling disease outbreaks, which according to the United States Department of Agriculture (USDA) cause $2.9–6.7 billion worth of losses every year [1]. Biosensors typically consist of a biological recognition layer (e.g. enzymes, antibodies, DNA etc.) integrated in proximity to a transducer which converts the binding event between the target and its specific probes into a measurable signal. For instance, in the most widely used enzyme-linked immunosorbent assay (ELISA) technique, the hybridization event between antibodies and antigen is reported using a colorimetric signal and with detection limits approaching picomolar range. Out of all detection methods used in biosensors, optical-based technique is the most popular one because of its high-sensitivity and its ability to remotely interrogate the information on the biosensor using light or laser. However, biosensors with electrical readouts offer several advantages over their optical counterparts due to their reduced cost, reduced form factor, and the ease of signal acquisition [2, 3]. One of the major challenges in the electrical or impedance based detection is low signal-to-noise ratio when compared to optical detection, which is attributed to the large magnitude of the background signal [3]. In this regard, a biomolecular amplification technique called "silver enhancement" could be ideal to boost the signal-to-noise ratio (SNR) of conductimetric biosensors to be comparable to that of its optical counterparts. In fact, silver enhancement has been previously proposed and used for improving the detection range in optical biosensors. In [4–7], silver enhancement has been used in conjunction with labeling with gold nanoparticles for optical detection in immunoassays. In [5], it was reported that the conjugation significantly increased

the detection limit of ricin to 100 pg/mL. We show in this paper that for conductimetric biosensors, silver enhancement significantly improves the SNR and in the process can achieve detection sensitivity comparable or better than an optical based system. Also, performing signal enhancement at the biomolecular level before performing electrical readout would reduce the effects of background interference [8–10].

The model conductimetric biochip used for this study has been constructed using functionalized gold nanoparticles on the high-density interdigitated microelectrode array. The interdigitated electrodes provide a large active area to facilitate binding between the analyte and the detection probe and hence have several advantages over non-interdigitated electrode arrays [11, 12]. The salient features of this study include: (a) a simple and robust electrical detection method using a combination of gold nanoparticle labels with silver amplification technique; (b) characterization of the extent to which the nanoparticle adsorption can be quantified using silver enhancement; (c) characterization of two distinct biomolecular transistor responses that are the sub-threshold and the above-threshold regions of the operation, and (d) characterization of the biochip sensitivity and the detection limit using repeated and controlled experiments. This paper is organized as follows: Sect. 2 describes the operating principle of the silver enhancement technique when applied to gold nanoparticles and the high-density microelectrode biochip. Section 3 describes the fabrication method of biochips and surface functionalization of biochips. Section 4 presents experimental results of detecting biomolecules using rabbit and mouse IgG as model antigen, which verify the principle of silver enhancement and the functionality of the biochip. Section 5 concludes with a brief discussion and the future work.

Biochip Architecture and Principle of Operation

The principle of conductimetric biochip detection is shown in Fig. 1 where initially probes specific to the target molecules are immobilized in the regions between two electrodes. When the analyte is applied, the target biomolecules interact with the specific probes. The secondary antibodies conjugated with gold (Au) nanoparticle are then applied to the biochip, which leads to the formation of a sandwich array as shown in Fig. 1a. This configuration is denoted as the "cutoff" region, since the current measured between the electrodes (for a fixed potential difference) is small. In the next step of the silver enhancement procedure, the active component (with gold nanoparticles) of the biochip is exposed to a solution of Ag (I) and hydroquinone (photographic developing solution). The gold nanoparticles act as a catalyst and reduce silver ions into metallic silver in the presence of a reducing agent (hydroquinone). The reduced silver then deposits on the gold surface, thus enlarging the size of the gold nanoparticles. As the size of the silver islands grows, they provide shorter paths for electrons to hop between the electrodes. The region of operation when the distance between the electrodes has not been fully bridged by the silver islands is the sub-threshold region (see Fig. 1b).With the increase in enhancement time, the consistent growth of silver-enhanced particles completely bridges the area between the electrodes. Under this condition, the device enters the above-threshold region of operation where a flow of current can be measured when a fixed potential is applied between the electrodes (Fig. 1c). The time required for the device to reach the threshold from the cutoff region is known as the transition time. In this paper, we use the sub-threshold and above-threshold characteristics of the device for conductimetric measurement of the concentration of the target biomolecules.

Biochip Fabrication and Surface Functionalization

The biochips were fabricated from 400 silicon wafers (p-type 100, thickness 500–550 μm). A 2-μm thick layer of thermal oxide was grown over the silicon to serve as an insulator between the electrodes and the substrate. Photolithography was used to pattern photoresist, metal electrodes were deposited by the evaporation of 10 nm of chrome under 100 nm of gold, and a lift-off process was used to develop the interdigitated electrode array. Figure 2 shows the high-density interdigitated electrodes biochip

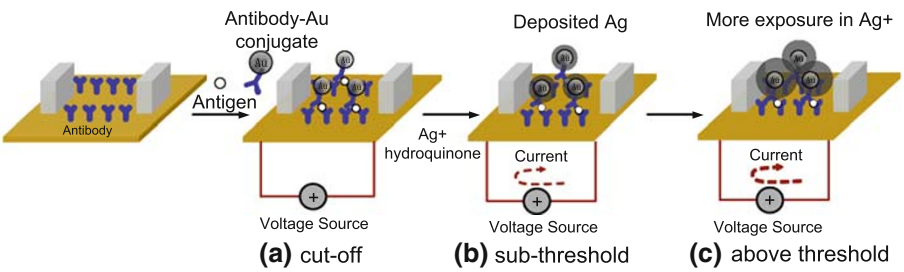

Fig. 1 The operating principle of the silver-enhanced biomolecular transistor with three distinct regions of the operation

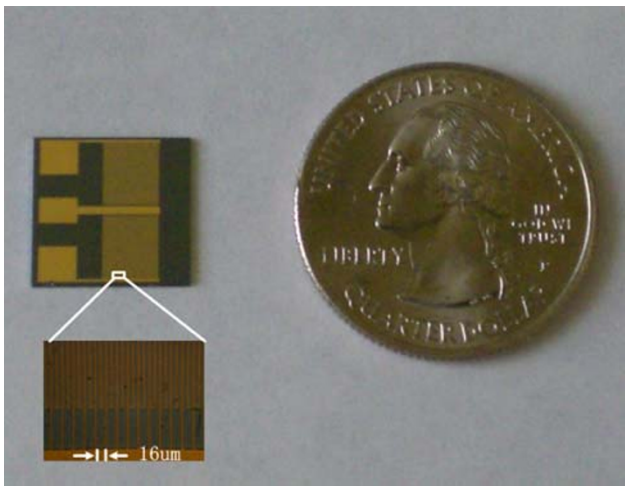

Fig. 2 The high-density interdigitated microelectrode biosensor

fabricated using a standard MEMS technology described above. Each electrode finger has a length of 5,000 μm, a width of 5 μm, and an inter-electrode spacing of 6 μm. The surface of biochips was then modified for immobilizing the antibody. The chips were first immersed in acetone in a crystallizing dish for 10 min to dissolve away the protective PR layer. The chips were then treated with 1:1 mixture of concentrated methanol and hydrochloric acid for 30 min followed by immersion into boiling distilled water for 30 min. The biochips were allowed to air dry completely. The cleaning and drying of the biochips are now ready for silanization where it occurred in an anaerobic glove box. The biochips were immersed in a crystallizing dish containing a solution of 2% 3-mercaptopropyltrimethyloxysilane (MTS) (Sigma; St. Louis, MS) for 2 h. The chips were then rinsed in toluene and allowed to dry completely. After silanization, *N*-y-maleimidobutyryloxy succinimide ester (GMBS) (Sigma; St. Louis, MA) was chosen as crosslinkers to avoid multi-protein complex [13]. The crosslinking reagent was dissolved in a minimum amount of dimethylformamide (DMF) and then diluted with ethanol to a final concentration of 2 mM. The silanized substrate was treated with crosslinker for 1 h and washed in phosphate buffered saline (PBS, pH 7.4). After the application of the crosslinker, antibody (Sigma; St. Louis, MA) was immobilized onto the biochip active surface. Figure 3 summarizes the process of biochip surface functionalization. The biochips were placed in a petri dish, sealed with parafilm, and allowed to incubate at 37°C for 1 h. The biochips were then treated with 2 mg/mL bovine serum albumin (BSA) (Sigma; St. Louis, MA) as blocking reagent for 45 min. After incubation, the biochip surface was rinsed with PBS (pH 7.4) and allowed to air dry. The confocal laser scanning microscopy image was used to validate antibody immobilization and determine where it occurred (Fig. 4). The image shows that the antibody immobilization was only occurring on the silicon dioxide area between the electrodes, thus proving the effectiveness of the surface functionalization.

Results and Discussions

Verification of the Operating Principle

The first step in verifying the silver enhancement principle is to measure the size of the silver-enhanced gold nanoparticles in the silver enhancer solution (Ted Pella, Inc., CA) with respect to the silver enhancing time. For this experiment, Zetasizer Nano (Malvern Instruments Ltd, UK) was used to characterize the particle size. Figure 5 shows the linear relationship between the silver enhancing time and the size of gold particles. We have observed that the 40-nm gold nanoparticles will reach average size of

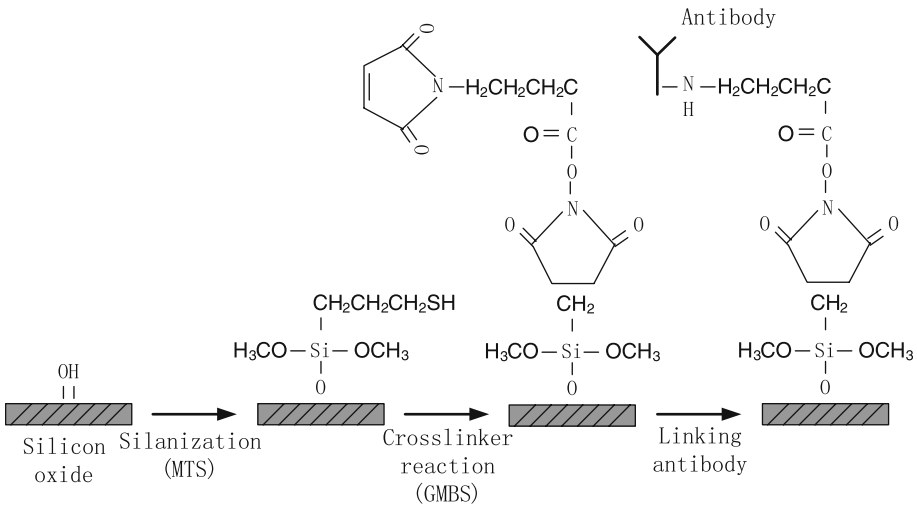

Fig. 3 The process of biochip surface functionalization

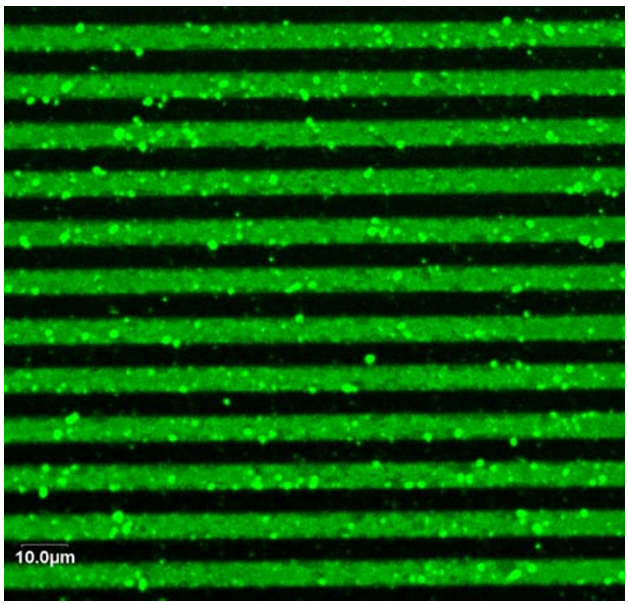

Fig. 4 Confocal laser scanning microscopy image of electrodes showing FITC-labeled bovine IgG only immobilized on silicon dioxide surfaces (*black areas* are the electrodes where no IgG are present)

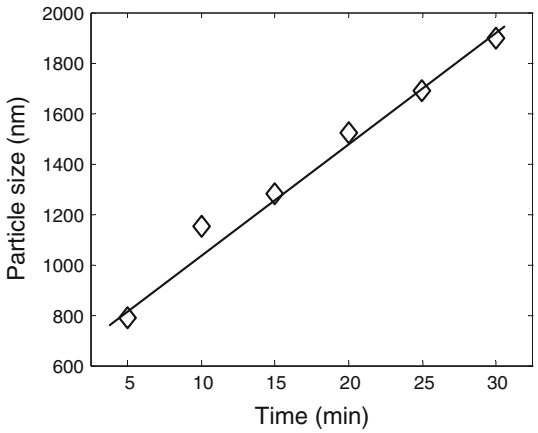

Fig. 5 The relationship between the silver-enhanced gold particle size and the silver enhancing time

1.2 μm when exposed to the silver enhancer for approximately 10 min. This interesting property makes the silver enhancement principle suitable for signal amplification in conductimetric biosensors.

To evaluate the detection capabilities of the biochip, we dispense 2.5 mM/mL gold anti-IgG conjugate onto the biochip surface for 1 h and then treat the biochip with silver enhancer solution (Ted Pella, Inc., CA). To stop silver enhancement, the biochip was rinsed with distilled water and was dried with N_2. Figure 6 shows the microscopic observations before and after 35 min silver enhancing time. As gold nanoparticles are 40 nm size and they can not be observed by in Fig 6a, where as they can be clearly observed after silver enhancement (see Fig. 6b). It can also be seen that the silver-enhanced gold particles form a bridge between the interdigitated electrodes. Figure 7 shows the SEM image of the bridge formed by silver-enhanced gold particles and then verifies the operating principle.

IgG Detection

Based on the principle of silver enhancement, we conduct IgG detection by first applying rabbit IgG onto the active

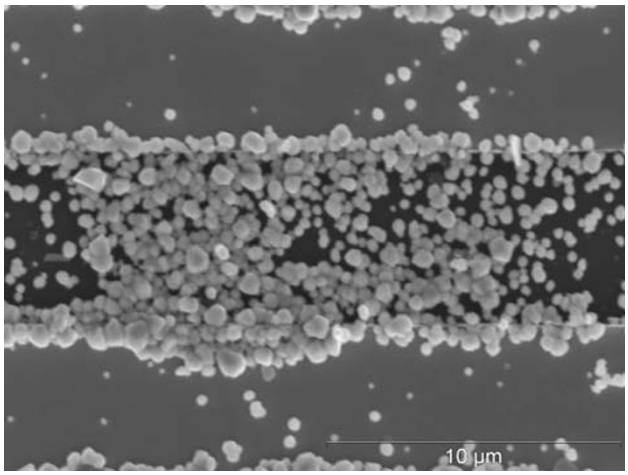

Fig. 7 SEM image of the bridge formed by enlarged gold particles

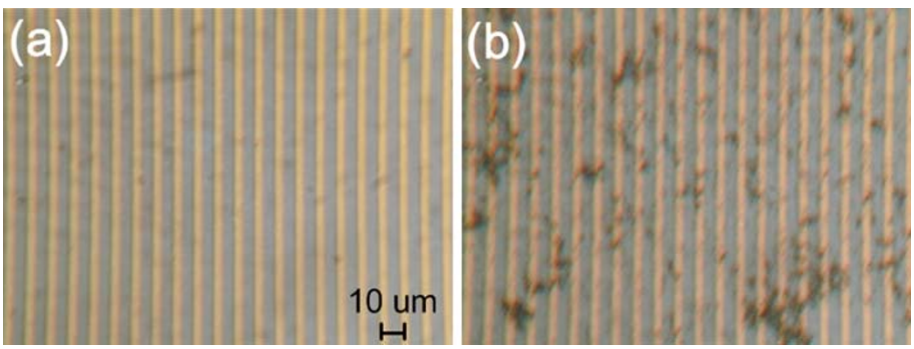

Fig. 6 Microphotographs for the biochip active surface. **a** before silver enhancement **b** 35 min after silver enhancement

area of the anti-rabbit IgG biochip allowing incubation for 30 min. Goat anti-rabbit IgG and gold conjugates were then applied and were incubated for 30 min. Excess gold conjugates were washed with PBS solution. Electrical measurements are taken after each treatment of the biochip with the silver enhancer solution, and the conductance between the electrodes was measured using a BK multimeter Model AK-2880A (Worchester, MA).

Figure 8 shows the conductance between the electrodes increases with the increasing exposure to the silver enhancer solution where the insert figure shows the conductance measurement in the logarithmic domain. The conductance increases when the biochip is exposed more in the silver enhancer solution as expected. It also clear shows the response has three distinct operation region (A, B, and C), which verifies the operating principle of the silver-enhanced gold nanoparticle-based biochip. During the sub-threshold region (labeled as B) of the operation, gold nanoparticles grow in the presence of silver enhancer solution thus leading to a shorter path for electron transport. But during this stage, enhanced gold particles have not formed the bridge to short the electrodes. With the increase in enhancement time, the consistent growth of silver-enhanced particles completely bridges the area between the electrodes, and there is immediate transition from state B to C when it happened (shown a step from B to C in the inserted figure in Fig. 8). In the stage C, more bridges formed by gold nanoparticles are building up in parallel, thus leading to more conductance increase until it become to a more stable state. Bovine IgG biochips were used as negative control experiments, and we have observed that the conductance of "control" biochip start to increase at 10 min. It means that the non-specific binding actually occurred, but the number of such events is much smaller than the number of specific binding events. Thus, the biochip is able to detect target IgG in the presence of background noise. We have seen that the measurement results are stable several days after the experiments have been conducted. Also, the results in Fig. 8 show that the detection range that can be achieved by proposed biosensor is 40 dB with respect to the control conductance.

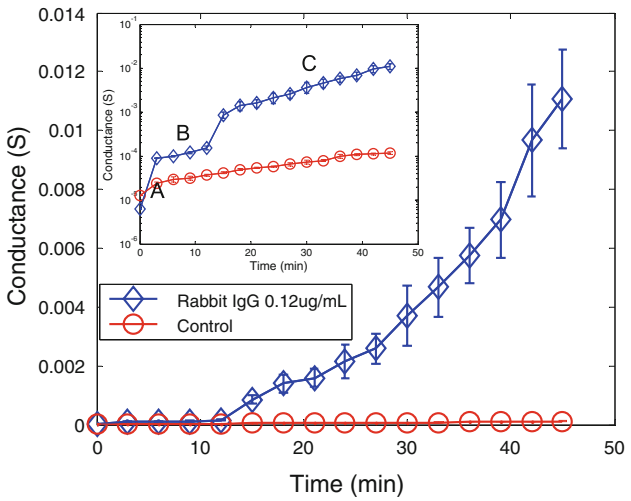

Fig. 8 Conductance of the biochips measured as a function of silver enhancing time. (*Inset*) Conductance measurement in logarithmic domain, which can clearly show that the biomolecular transistor exhibits three different types of responses (labeled as *A*, *B*, and *C*) based on the nature of the conductive path across the electrodes. *A* cutoff region; *B* sub-threshold region when the formation of the conductive bridge between the electrodes is incomplete; *C* above-threshold region where the bridge is completely formed by silver-enhanced gold nanoparticles leading to a step increase in conductance and conductance slope

We also conducted rabbit IgG detection using different IgG concentrations, and Fig. 9 shows the conductance measurements at 45 min with three IgG concentrations and the control experiment. For each concentration, the experiment is repeated three times, and the standard deviation is also shown in the graph. It clearly shows that pathogenic and non-pathogenic cases can be easily distinguished even with low concentration of IgG. As seen in the graph, the conductance of biochip decrease with the decrease of the IgG concentration level, implying a decreasing of the signal-to-noise ratio. Similar experiments have been performed using anti-mouse IgG biochip with the mouse IgG detection, and the results are shown in the Fig. 10. These repeated and controlled experimental results verify the functionality of proposed biochip to detect biomolecules.

Some researchers have argued that the conductivity-based silver-enhanced detection is not applicable to quantitative concentration assays, because the electrodes are short circuited above a certain density of the silver-enhanced gold particles [4]. In the next experiment, we will show that the quantitative analysis can be achieved by adjusting silver enhancing time. Figure 11 shows the

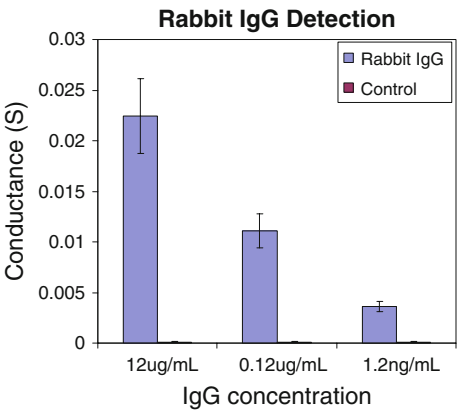

Fig. 9 Steady state conductance measurement of rabbit IgG detection

Fig. 10 Steady state conductance measurement of mouse IgG detection

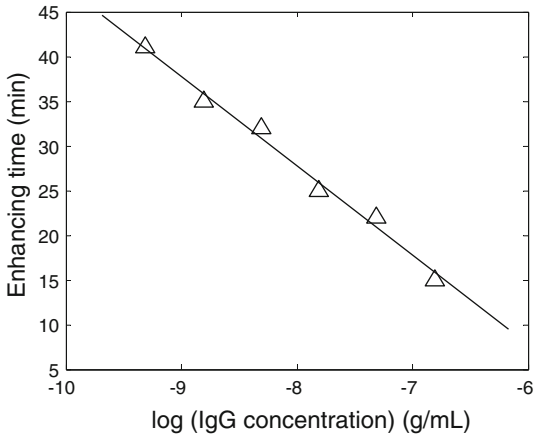

Fig. 11 Quantitative analysis: the silver enhancing time required to reach a conductance range of 3.8–5 mS as a function of IgG concentrations

relation of the silver enhancing time required to reach a conductance range of 3.8–5 mS as a function of rabbit IgG concentration. It is interesting to note that 240 pg/mL rabbit IgG can be detected when the conductance increases to 3.8 mS at the silver enhancing time of 42 min.

We have shown the experiments to verify the principle of silver-enhanced electrical detection of biomolecules using rabbit IgG as model antigen. One issue that other researchers have not addressed in the silver enhancement method is the accuracy and possible false positive errors. Due to the sensitivity of the presence of gold nanoparticles when exposing to silver, it might have a high level of false positive results. The typical method of prevention is to extensively wash the biochips to alleviate non-specific binding. However, the method is time consuming, and it is not always effective. Another alterative solution is to embed the biochip with error-correction function by employing encode-decoding scheme similar to the approach that we have previously reported [14].

Conclusions

In this paper, we have designed and characterized a silver enhancement technique for amplifying the signal for gold nanoparticle label at biomolecular level. The gold nanoparticles serve as nucleation sites about which a reduction reaction deposits silver and hence enlarges the size of the gold nanoparticle. Using silver enhancer solution, the gold antiparticles can grow into a micro size particle and ultimately can bridge the gap between electrodes, leading a measurable change in conductance. Comprehensive experiments have verified the effectiveness of surface functionalization and the functionality of biochip. The proposed biochip in conjunction with silver enhancement provides a simple, effective, and sensitive way of detecting trace quantity of biomolecules.

Acknowledgments This work is supported in part by a research grant from the National Science Foundation: NSF ECCS-0622056. Authors also would like to thank Lurie Nanofabrication Facility at University of Michigan for the fabrication of biochips.

References

1. Food and Drug Administration, *Bacteriological analytical manual*, 8th edn. (Association of Analytical Chemists, Arlington, VA, 2000)
2. Y. Liu, A. Gore, S. Chakrabartty, E. C. Alocilja, Microchimica Acta **163**, No. 1–2, 49–56 (2008)
3. J.-H. Kim, J.-H. Cho, S.C. Geun, C.-W. Lee, H.-B. Kim, S.-H. Peak, Biosensors Bioelectron. **14**, No. 12, 907–915 (2000)
4. S. Gupta, S. Huda, P.K. Kilpatrick, O.D. Velev, Anal. Chem, **79**, No. 10, 3810–3820 (2007)
5. R.H. Shyu, H.F. Shyu, H.W. Liu, S.S. Tang, Toxicon **40**, No. 3, 255–258 (2002)
6. O.D. Velev, E.W. Kaler, Langmuir, **15**, No. 11, 3693–3698 (1999)
7. K.T. Liao, H.J. Huang, Anal. Chim. Acta **538**, No. 1–2, 159–164 (2005)
8. M. Li, Y.C. Lin, K.C. Su, Y.T. Wang, T.C. Chang, H.P. Lin, Sens. Actuators B **117**, 451–456 (2006)
9. R. Porter, P. van der Logt, S. Howell, M.K. Reay, A. Badley, Biosens. Bioelectron. **16**, 875–885 (2001)
10. R.Q. Liang, C.Y. Tan, K.C. Ruan, J. Immunol. Methods **285**, 157–163 (2004)
11. S.J. Park, T.A. Taton, C.A. Mirkindagger, Science, **295**, No. 5559, 1503–1506 (2002)
12. C.H. Yeh, H.H. Huanga, T.C. Chang, H.P. Lin, Y.C. Lin, Biosens. Bioelectron. **24**, 1661–1666 (2009)
13. S.K. Bhatia, L.C. Shriver-Lake, K.J. Prior, J.H. Georger, J.M. Calvert, R. Bredehorst, F.S. Ligler, Anal. Biochem. **178**(2), 408–413 (1989)
14. Y. Liu, S. Chakrabartty, E.C. Alocilja, Nanotechnology, **18**, No. 42, 424017 (2007)